Response of a Fermi gas in a disordered system to a phonon flux

D. Poplavsky and B. Danilchenko
Institute of Physics of the National Academy of Sciences of Ukraine, Prospect Nauki 46, 252650 Kiev, Ukraine

H. Kostial
Paul-Drude-Institut für Festkörperelektronik, Hausvogteiplatz 5-7, D-10117 Berlin, Germany
(Received 23 September 1999)

Phonon-induced conductivity (PIC) in a strongly elastically scattered two-dimensional electron gas in δ-doped GaAs was studied using the heat-pulse technique. The results of phonoconductivity behavior with carrier temperature as well as magnetic field are presented. It was established that PIC is due to the influence of phonon flux on the temperature-dependent quantum corrections to conductivity through carrier heating. It was shown that the value of PIC is determined both by the absorbed nonequilibrium phonon power and the energy losses to lattice. The value of phonon flux energy absorbed by carriers was estimated from experiment.

I. INTRODUCTION

Low-dimensional electronic systems have been under intensive investigations for many years. The properties of such systems crucially depend on the presence of disorder that gives rise to some new fundamental phenomena. Depending on how strong the disorder is, the electronic system can be in the weakly localized (WL) or the strongly localized transport regimes.[1] In the WL regime, carriers are strongly elastically scattered and move diffusely. As a result of the constructive interference of counterpropagating scattered electron waves a negative correction to conductivity appears. This effect exists only if $\tau \ll \tau_\varphi$, where τ is the elastic scattering and τ_φ is the phase-breaking time, respectively. The latter is determined by nonelastic processes of carrier scattering and can also be governed by application of an external magnetic field.[1,2] For the two-dimensional electron gas (2DEG) this correction to conductivity logarithmically depends on temperature.

Phonon-assisted processes under the presence of a strong electron-electron interaction change the temperature of carriers and, hence, effect the value of the conductivity correction. For this reason, if electron-electron collisions are much faster than electron-phonon processes, then one can expect an increase of electron temperature and hence a conductivity change to be caused by absorption of phonons. Theoretical studies for 1DEG performed by Blencowe[3] showed that disorder effects (electron-electron interaction in the dirty limit and weak localization) play an essential role in the phonon-induced conductivity and may lead to positive sign of phonoconductivity (PC). Recently the experimental observation of positive phonoconductivity response to the phonon flux was realized in 1DEG by Kent *et al.*[4] It was pointed out that the destruction of weak localization by nonequillibrium phonons can be the most important factor in the formation of positive response.

Nevertheless until now there has been no direct experimental evidence of the nature positive phonoconductivity response. Moreover, it is important to establish the relation between observed phonoconductivity response and the set of basic parameters of the electronic system that include efficiency of phonon absorption, energy relaxation rate, and phase-breaking time.

Ideal objects for the study of weak localization effects are quasi-2D δ-doped structures, where the 2D electron (hole) gas is created by doping of one atomic plane by donor (acceptor) atoms. Such structures are characterized by strong carrier scattering on impurities, which leads to a strongly pronounced weak localization effect.[5,6]

In this article we report the experimental evidence that the positive phonoconductivity in the typical disordered electronic system, δ-doped GaAs, is mainly due to the destruction of weakly localized electronic states by incident phonon flux. This provides an experimental method for studying the electron-phonon interaction in low-dimensional disordered electronic systems.

The article is organized as follows. The experimental setup is described in Sec. II. Main experimental results of phonoconductivity and transport measurements are reported in Sec. III. In Sec. IV we present a physical model for experimentally observed positive phonoconductivity. Section V is dedicated to detailed description of the calculation of phonon-absorbed power in the δ-doped structure. The results of calculations and their comparison with experiment are discussed in Sec. VI. Conclusions are presented in Sec. VII.

II. EXPERIMENTAL DETAILS

The two-dimensional electron gas was formed in molecular beam epitaxially (MBE) grown silicon δ-layers embedded into a GaAs matrix. The substrate was (001) semi-insulating GaAs with thickness of 3.4 mm. The structure consisted (beginning from the substrate) of 1 μm buffer layer, seven δ-layers with donor concentration 5×10^{11} cm^{-2} per layer, separated by 100 nm, 150-nm spacer layer, and 150-nm cap layer with 1×10^{17} cm^{-3} impurity atoms. A 0.3×0.34 mm^2 area of 2DEG was supplied by Au:Ge ohmic contacts alloyed at 430 °C in N_2/H_2 atmosphere.

On the side opposite to the 2DEG, a 1×1 mm^2 Au heater

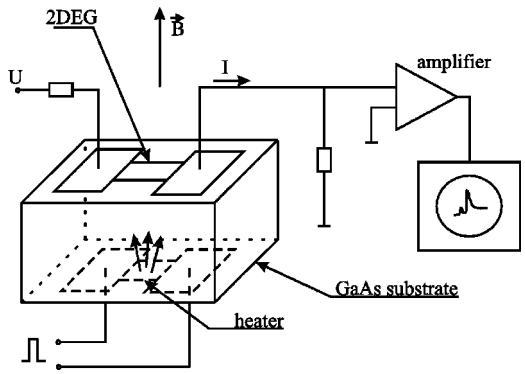

FIG. 1. Scheme of experiment.

film was deposited center-to-center to the 2DEG structure. It had an impedance of approximately 50 Ω for better matching with coaxial cable. Nonequilibrium phonons were generated by $\tau_{\text{pulse}}=75$ ns voltage pulses applied to the heater. Phonons, injected into the crystal, propagated to 2DEG and increased its conductivity. The sample geometry and mutual positions of phonon source and studied 2DEG are shown in Fig. 1.

The phonon-induced current change was measured as a voltage drop across a 50-Ω resistor connected in series with the structure when a constant bias voltage was applied to the sample. This voltage drop was detected by means of a high-speed digital oscilloscope. In order to exclude the effect of synchronous crosstalk from heater excitation pulse the signals were recorded as the difference between the signals for positive and negative polarity biases. Signals were accumulated approximately 10^3 times to get the appropriate signal/noise ratio. The sample thickness was large enough to resolve different phonon modes in time.

The sample was immersed in liquid helium at temperatures 2–4.2 K and in helium vapor at higher temperatures. All results presented in this paper were obtained for the highest power dissipated in the heater of approximately 7×10^3 W/cm^2, except the dependence of phonoconductivity on heater temperature (see Sec. III, Fig. 5). The indicated power corresponds to heater temperature $\simeq 18$ K if calculated from acoustic mismatch theory for ambient temperature $T=2$ K:

$$T_h=\sqrt[4]{T^4+\sigma P}, \tag{1}$$

where P is the power dissipated in the heater and σ is a constant defined in Ref. 7. We did not observe any drop in the signal at the crossover between liquid/vapor ($T=4.2$ K) and normal/superfluid ($T=2.17$ K) helium, which means that the power dissipated in the heater was large enough to cause the boiling of helium around the heater film (for highest power as given above). Therefore we can assert that in the whole range of ambient temperatures the heater film was surrounded by helium vapor. This conclusion is also in correspondence with results of Ref. 8.

III. EXPERIMENTAL RESULTS

Experimental time-resolved phonoconductivity spectra are presented in Fig. 2. One can see that both longitudinal (LA) and transversal (TA) acoustical modes are fully resolved in time due to the large enough thickness of the substrate. The arrival times of different phonon modes are determined by corresponding sound velocities. This figure also shows the behavior of phonoconductivity with carrier heating caused either by electric field [Fig. 2(a)] or by ambient temperature [Fig. 2(b)]. It is clearly seen that phonoconductivity decreases with increasing carrier temperature. The value of phonon-induced change of conductivity appeared to be of the order of 1% of 2DEG dc conductivity at nonheating electric field [$\sigma(4.2\text{ K})=0.2$ mS/square].

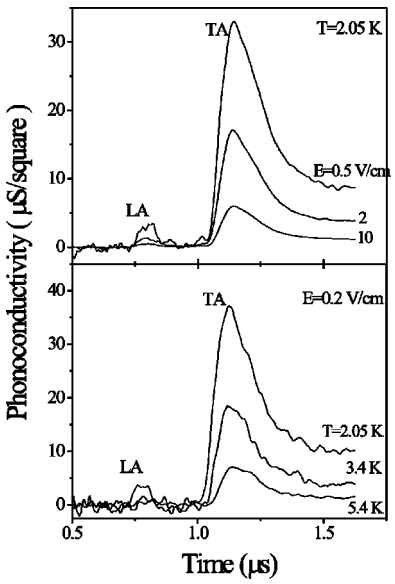

FIG. 2. The typical time-traced phonoconductivity signals for different temperatures and electric field strengths.

The dependence of phonoconductivity on supplied electric power (measured at the lowest temperature) and temperature (measured at nonheating electric field) is shown in Fig. 3(a). The dependence plotted in Fig. 3(a) is for the TA phonon mode, the behavior for the LA mode is similar, but the accuracy for this phonon mode was lower. The depen-

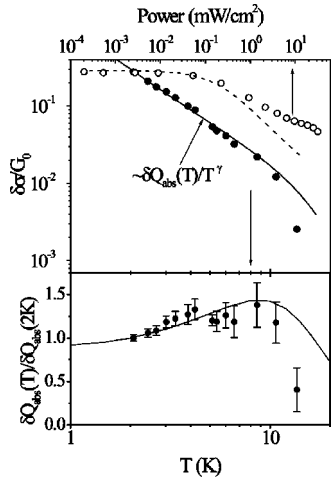

FIG. 3. (a) The dependence of phonoconductivity response on temperature (●) and heating electric power (○). Solid and dashed lines represent calculations according to Eq. (9) and Eq. (32) with $\gamma=2$. (b) The temperature dependence of absorbed phonon power deduced from experiment (●) and calculated (solid line).

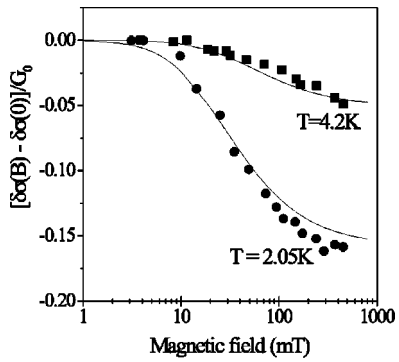

FIG. 4. Magnetic field dependence of phonon-induced conductivity for different temperatures. Solid lines represent calculations according to Eq. (10) for $C'=1.4$.

dence on electric power can be divided into the region where phonoconductivity is almost independent on input electric power (nonheating region) and the region with decreasing phonoconductivity. The latter corresponds to the case when the electrons are already significantly heated by applied electric field.

Figure 4 shows the dependence of phonoconductivity on external magnetic field applied perpendicular to the 2DEG plane. Measurements were carried out at two different temperatures and nonheating electric fields. This figure shows that the value of phonoconductivity decreases with increasing magnetic field. It is worth noting that while the absolute value of the ''magnetophonoconductivity'' decreases with increasing temperature, the relative changes are almost the same at different temperatures—the phonoconductivity is two times smaller at $B=500$ mT comparing to its value at zero magnetic field.

The dependence of phonoconductivity on heater temperature for constant ambient temperature $T=2$ K is shown in Fig. 5. These results were obtained for a nonheating bias electric field applied to the 2DEG. The heater temperature was calculated according to acoustic mismatch theory [see Eq. (1)]. One can see that the phonon signal grows together with growing heater temperature, which determines the total phonon flux incident to the 2DEG. This figure also shows the result of calculation (solid line) discussed in Sec. VI.

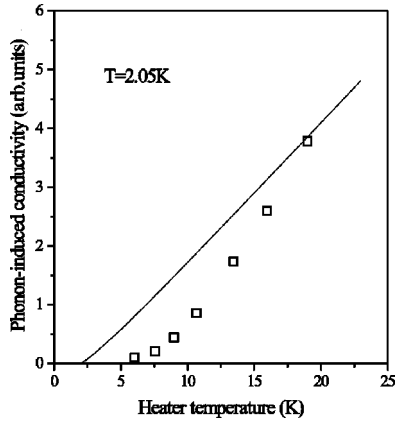

FIG. 5. Phonoconductivity vs heater temperature at the constant ambient temperature $T=2.05$ K. Squares are the experimental data, solid line, the calculation.

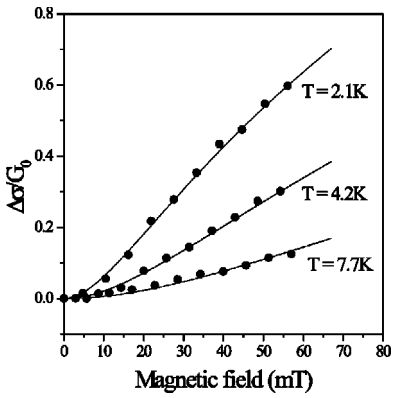

FIG. 6. Magnetoconductivity in a perpendicular magnetic field at different temperatures. Circles correspond to experimental data, solid lines are fits according to Eq. (2).

The measurements of magnetoconductivity in the temperature range 2–15 K proved the presence of weak localization in the system under investigation. Figure 6 shows the experimental results of these measurements along with theoretical calculations according to the existing theory of weak localization.[9] For 2DEG magnetoconductivity is described by the following formula:[9]

$$\sigma(B)-\sigma(0)=\alpha G_0 F\left(\frac{4De\tau_\varphi}{\hbar}B\right), \tag{2}$$

where α is a coefficient of the order of unity, $G_0=e^2/(2\pi^2\hbar)$, D is the electron diffusion coefficient, τ_φ the phase-breaking time, B the magnetic field, $F(x)=\ln x+\psi(1/2+1/x)$, and $\psi(x)$ the digamma function. Using this formula to fit experimental magnetoconductivity at different temperatures one can obtain the temperature dependence of fitting parameters α and τ_φ. We found that $\alpha\simeq 0.8$ and does not depend on temperature, and $\tau_\varphi \propto T^{-1}$ (see Fig. 7). The latter indicates that the Nyquist phase relaxation mechanism is dominant in our system, which is consistent with previous investigations on $\delta\langle\mathrm{Si}\rangle$-GaAs systems.[5,6]

The carrier temperature can be varied not only by changing the ambient temperature but also by increasing the heating electric field applied to the 2DEG. In the latter case the Joule power, supplied to carriers, heats them up. When the

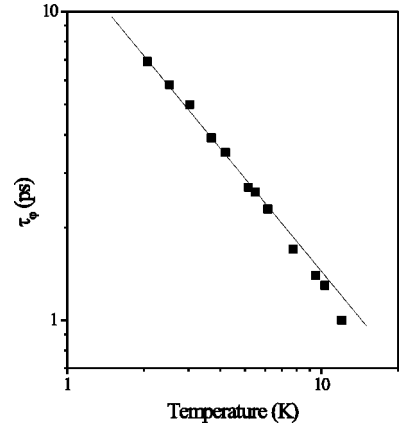

FIG. 7. Phase-breaking time τ_φ vs ambient temperature. Straight line represents T^{-1} fit.

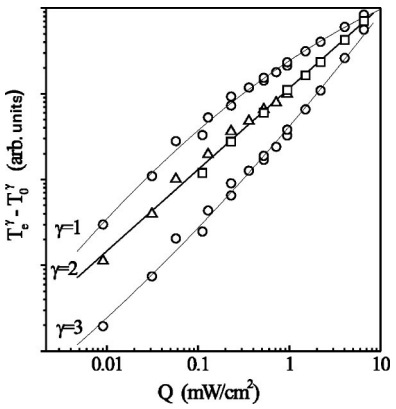

FIG. 8. Energy loss rate by hot carriers in different representations. Experimental data are shown by points. For $\gamma=2$, squares, data obtained from the temperature dependence of conductivity; triangles, from magnetoconductivity.

Joule power is supplied in a steady regime (which is our case) then the temperature of carriers T_e is different from the ambient temperature T ($T_e > T$). In the range of electric field strengths reached in the experiment (up to 20 V/cm) the heating of the lattice was negligibly small, which was confirmed by the fact that I-V curves measured in a steady-state regime and in ns-pulse regime ($\tau=30$ ns) were identical. Experimental magnetoconductivity curves at different heating electric fields E are well fitted according to Eq. (2). Then comparing the dependence of τ_φ on temperature and Joule power one can determine the dependence of electron temperature T_e on supplied electric power $Q=\sigma E^2$. The alternative way is to compare the dependence of steady-state conductivity on temperature (at low electric field) and Joule power (at the lowest temperature).[11] The dependence is plotted then in the following form:

$$T_e^\gamma - T^\gamma = \beta Q, \tag{3}$$

where β is a coefficient and γ a positive number determined both by the dimensionality of the electron gas and the mechanism of electron-phonon coupling. This dependence for various values of γ is plotted in Fig. 8. One can see that the best value is $\gamma=2$. The value of coefficient β for $\gamma=2$ is $\beta=15\times10^3$ K^{2}cm^2/W. The result $\gamma=2$ agrees with earlier experiments performed for higher concentrations of electrons in the same structures.[5] This result corresponds to energy losses via piezoacoustical phonon coupling in the 2DEG with several occupied subbands, which first were studied for a AlGaAs/GaAs heterojunction in Ref. 11. In this case energy losses go mainly through higher subbands, where carriers are less confined than in lower subbands.[11]

IV. GENERAL MODEL FOR PHONON-INDUCED CONDUCTIVITY

We assume that positive phonoconductivity appears due to the increase of electron temperature under the absorption of incident phonon flux. This assumption is valid only if the time of electron-phonon interaction is much greater than the time of electron-electron collisions, i.e., $\tau_{\text{e-ph}} \gg \tau_{e\text{-}e}$. This means that if one electron absorbs a phonon, then the additional energy of this electron is distributed very quickly among all electrons well before the system will lose this energy via a phonon emission event. This condition is fulfilled in the studied system since the characteristic time of electron-electron interaction is found to be of the order of 1 ps (see Fig. 7), while the time of electron-phonon interaction is greater at least by two to three orders of magnitude. Temperature rise due to phonon absorption decreases the value of quantum correction to conductivity (contributed from both WL and electron-electron interactions), which means that the conductivity of the whole system increases. Therefore one should observe positive phonoconductivity responses that were really observed in the experiments discussed in this paper.

Along with a qualitative description of the observed phonoconductivity it is possible to find a quantitative approach to this phenomenon. The formula for the temperature dependence of quantum correction to conductivity in the 2DEG is[1]

$$\Delta\sigma(T) = C' G_0 \ln(kT\tau/\hbar), \tag{4}$$

where τ is the elastic scattering time, $C' = p + (1-p)\beta + \Lambda$, and p the exponent of the temperature dependence of phase-breaking time ($\tau_\varphi \propto T^{-p}$, with $p=1$, see Fig. 7), β is the Maki-Thompson parameter, and Λ a parameter of electron-electron interaction. If the change of electron temperature is small compared to the equilibrium temperature ($\delta T \ll T$) then the induced conductivity can be written as a variation of $\Delta\sigma$ with respect to temperature. Finding the derivative of Eq. (4) and multiplying by δT one obtains

$$\frac{\delta\sigma(T)}{G_0} = C' \frac{\delta T}{T}. \tag{5}$$

In order to establish the temperature dependence $\delta\sigma(T)$ one has to find the phonon-induced temperature rise δT, which in general depends on the ambient temperature. The process of the absorption of phonon flux emitted from the heater into the crystal can be considered as a steady-state case. It is a valid approach because the duration of phonon pulse ($\tau_{\text{pulse}}=75$ ns) is much greater than the time of electron-phonon interaction ($\tau_{\text{e-ph}} \sim 1$ ns). This means that during the time τ_{pulse} which phonon pulse goes through the electron system, electrons are heated very quickly (of the order of $\tau_{\text{e-ph}}$) to the temperature $T+\delta T$ and after that all absorbed energy is being emitted back into the lattice. This case is similar to the process of heating of electrons by direct electric current: all electric power is emitted to the lattice and the temperature of electrons is higher than the lattice temperature. Therefore we can employ the steady-state balance equation for the considered case

$$\delta Q_{\text{abs}}(T) = \delta Q_{\text{emit}}(T, \delta T), \tag{6}$$

where $\delta Q_{\text{abs}}(T)$ is the absorbed phonon power and $\delta Q_{\text{emit}}(T, \delta T)$ the emitted phonon power. The absorbed phonon power, or the rate of phonon flux absorption by 2D electrons, is determined mainly by electron-phonon matrix elements and energy distribution of phonons in the incident phonon flux; it will be considered in detail in Sec. V. The emitted phonon power, or the energy loss rate by 2D electrons, is a characteristics of the 2DEG only. This quantity

shows how fast electrons lose their energy when their temperature is above the equilibrium temperature of lattice. The energy loss rate has already been determined experimentally in Sec. III, see Fig. 8 and Eq. (3). In order to determine the value of $\delta Q_{\mathrm{emit}}(T,\delta T)$, one should find the derivative of Eq. (3) with respect to the electron temperature T_e,

$$\gamma T^{\gamma-1}\cdot\delta T=\beta\delta Q_{\mathrm{emit}}(T,\delta T), \tag{7}$$

with $\gamma=2$ for the studied system. Then, expressing the temperature change δT and using Eq. (6) we obtain the expression for δT,

$$\delta T=\frac{\beta}{\gamma}\frac{\delta Q_{\mathrm{abs}}(T)}{T^{\gamma-1}}. \tag{8}$$

Therefore substituting this formula into Eq. (5) we obtain the final expression for temperature-dependent phonoconductivity

$$\frac{\delta\sigma(T)}{G_0}=A\frac{\delta Q_{\mathrm{abs}}(T)}{T^{\gamma}}, \tag{9}$$

where $A=C'\beta/\gamma$. This formula includes the temperature dependent absorbed phonon power $\delta Q_{\mathrm{abs}}(T)$, which will be considered in Sec. V.

In order to establish the dependence of phonoconductivity on the perpendicular magnetic field (shown in Fig. 4) the same variation procedure must be employed. The variation with respect to temperature should be applied to Eq. (2) where the phase-breaking time τ_φ depends on temperature ($\tau_\varphi\propto T^{-1}$). After simple transformations we obtain the following expression:

$$\delta\sigma(B,T)-\delta\sigma(0,T)=\frac{\alpha}{C'}\delta\sigma(0,T)x(T)g[x(T)], \tag{10}$$

where $x(T)=4De\tau_\varphi(T)B/\hbar$, and $g(x)=-dF(x)/dx$. This expression can be used directly to fit experimental data of magnetic field dependence of phonoconductivity with one adjustable parameter C'. The result for two different temperatures is presented in Fig. 4 by solid lines. This fitting procedure was applied only for the low magnetic field region (up to 100 mT), where the contribution from electron-electron interaction in diffusion channel[9,10] to magnetoconductivity was small and magnetoconductivity results were adequately fitted according to WL theory [see Eq. (2) and Fig. 6]. The value of parameter C' is equal to 1.4 for both temperatures. Taking into account the expression for parameter C' [see Eq. (4)] for the particular case $p=1$ in the studied system, it is possible to estimate the constant of electron-electron interaction Λ. We have $C'=1+\Lambda$, therefore $\Lambda=0.4$.

Now we are able to estimate the change of electron temperature δT according to Eq. (5), which gives the highest value (for the lowest temperature $T=2$ K) $\delta T\simeq 0.4$ K. This result confirms the validity of our approach since it is based on the assumption $\delta T\ll T$, as was already indicated above.

V. THEORY

A. Electron wave functions and energy levels

The calculation of phonon power absorbed by 2D electrons requires the calculation of electron wave functions and energy structure of the 2DEG for arbitrary temperature. All the calculations related to the electronic structure of the δ layer were performed for nonzero temperature. However the effect of the temperature on wave functions and energy levels of the electron system had a negligible contribution to calculated absorbed phonon power in the studied temperature range (2–20 K). Therefore we exclude its effect from wave functions and energy level positions, and use expressions for $T=2$ K. It is supposed that donor atoms are uniformly distributed strictly in the x-y plane, i.e., their distribution function in the z direction (perpendicular to the plane) has the following form

$$N_d(z)=N_s\delta(z), \tag{11}$$

where N_s is the sheet concentration of donor atoms. The concentration of background acceptors is small compared to the corresponding bulk concentration of donors; therefore the presence of an acceptor background is neglected in the calculations.

The electron wave functions are written in the form of plane waves in an x-y plane and envelope function in the z direction:

$$\Psi_{\nu,\vec{k}_{||}}(\vec{r},z)=\frac{1}{\sqrt{A}}\psi_\nu(z)\exp(i\vec{k}\vec{r}), \tag{12}$$

where ν is the subband index, $\vec{k}$ the electron wave vector in an xy plane, $\vec{r}$ the electron radius vector in an x-y plane, $\psi_\nu(z)$ the electron envelope wave function in the z direction, and A the sample area. The electron energy spectrum is parabolic and can be written as

$$E_\nu(\vec{k})=E_\nu+\frac{\hbar^2k^2}{2m^*}, \tag{13}$$

where E_ν is the energy position of the νth subband, m^* is the electron effective mass ($m^*=0.067m_0$ for GaAs).

The way to determine the electronic structure of a δ-doped system is to solve self-consistently the one-dimensional Shrödinger equation for an envelope wave function and Poisson equation for confinement potential.

The Shrödinger equation has the form

$$-\frac{\hbar^2}{2m^*}\frac{d^2\psi(z)}{dz^2}+[V(z)-E]\psi(z)=0, \tag{14}$$

where $V(z)=V_1(z)+V_2(z)$ is the effective confinement potential that includes the self-consistent potential $V_1(z)$ and the exchange-correlation potential $V_2(z)$. The self-consistent potential satisfies the Poisson equation

$$\frac{d^2V_1(z)}{dz^2}=\frac{4\pi e^2}{\kappa}[N_s\delta(z)-n(z)], \tag{15}$$

where κ is the dielectric constant ($\kappa=12.8$ for GaAs), and $n(z)$ the electron density. The exchange-correlation potential

$V_2(z)$ was taken in the form of a parametrized expression given by Perdew and Zunger[12] (see also Ref. 13).

The electron density in the νth energy subband is determined by

$$n_\nu = \int_{E_\nu}^{\infty} D(E) f_T(E) dE, \tag{16}$$

where $D(E) = m^*/(\pi\hbar^2)$ is the two-dimensional electron density of states, and $f_T(E) = \{1 + \exp[(E-\mu)/k_B T]\}^{-1}$ is the Fermi-Dirac distribution. The total sheet density of 2D electrons is then

$$n = \sum_\nu n_\nu, \tag{17}$$

and the 3D electron density is calculated from

$$n(z) = \sum_\nu |\psi_\nu(z)|^2 n_\nu. \tag{18}$$

Results of numerical calculations showed that for the studied concentration of donors ($N_s = 5\times10^{11}$ cm^{-2}) only two energy subbands are filled with electrons. The first subband contains 87% of electrons and lies at $E_1 = -17.7$ meV; the second subband contains 13% of carriers and its energy position is $E_2 = -5.1$ meV. The value of the chemical potential is $\mu = -2.9$ meV. Here zero energy level corresponds to the bottom of a 3D conduction band and all figures are for $T = 2$ K.

B. Electron-phonon interaction and phonon-flux-absorbed power

We now turn to the electron-phonon interaction in δ-doped GaAs layers and our final task here is to calculate the phonon power absorbed by 2D electrons. Let us start with the electron-phonon interaction first. According to the ''Fermi golden rule'' the probability of electron transition with absorption of a phonon with wave vector $\vec{q}$ and polarization λ is determined by

$$\Gamma_\lambda(\vec{q},T) = 2\frac{2\pi}{\hbar} \sum_{\nu,\vec{k},\nu',\vec{k}'} |M_{\nu\nu',\lambda}(\vec{k},\vec{k}';\vec{q})|^2 f_T(E_{\vec{k}}) \times [1 - f_T(E_{\vec{k}'})]\,\delta(E_{\vec{k}'} - E_{\vec{k}} - \hbar\omega_{\vec{q}}), \tag{19}$$

where $|\nu,\vec{k}\rangle$ and $|\nu',\vec{k}'\rangle$ are the initial and final electron states, $\omega_{\vec{q}}$ is the phonon frequency (we consider long-wavelength phonons, i.e., $\omega_{\vec{q}} = c_\lambda q$, where c_λ is the sound velocity), and the screened matrix element $M_{\nu\nu'}(\vec{k},\vec{k}';\vec{q})$ is given by

$$M_{\nu\nu',\lambda}(\vec{k},\vec{k}';\vec{q}) = \sum_\beta \varepsilon^{-1}_{\alpha,\beta}(q_\parallel) M^{(0)}_{\beta,\lambda}(\vec{k},\vec{k}';\vec{q}), \tag{20}$$

where $\alpha = (\nu,\nu')$, $\beta = (\mu,\mu')$, sum $\beta = (\mu,\mu')$ runs over all energy subbands of the considered system, $\varepsilon_{\alpha,\beta}(q_\parallel) = \varepsilon_{(\nu\nu')(\mu\mu')}(q_\parallel)$ is the matrix dielectric function (derived in Appendix A) and the unscreened matrix element is given by

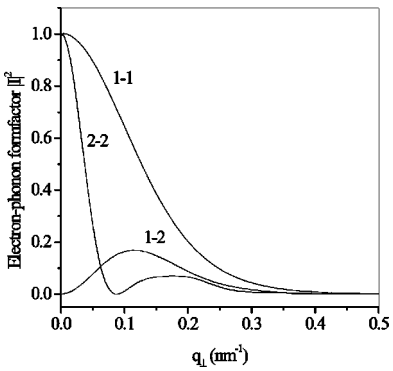

FIG. 9. Electron-phonon form factors for first and second subbands.

$$M^{(0)}_{\nu\nu',\lambda}(\vec{k},\vec{k}';\vec{q}) = \left(\frac{\hbar}{2\rho\omega_q V}\right)^{1/2} M_\lambda(\vec{q}) I_{\nu\nu'}(q_\perp)\,\delta_{\vec{k}-\vec{k}',\vec{q}_\parallel}, \tag{21}$$

where ρ is the mass density, V the volume, $q_\perp$ and $q_\parallel$ are the projections of the phonon wave vector to the z axis and the 2DEG plane, respectively. The piezoacoustic electron-phonon interaction has the form[14]

$$|M_\lambda(\vec{q})|^2 = (eh_{14})^2 A_\lambda, \tag{22}$$

where the constant of the piezoacoustic interaction $h_{14} = 1.2\times10^7$ V/cm and A_λ is defined by [for the (001) channel]

$$A_\lambda = \frac{9}{2}\frac{c_T}{c_L}\frac{q_\perp^2 q_\parallel^4}{q^6} \quad \text{for LA mode,}$$

$$A_\lambda = 4\frac{q_\perp^4 q_\parallel^2}{q^6} + \frac{1}{2}\frac{q_\parallel^6}{q^6} \quad \text{for TA mode,}$$

where $c_T = 3.03\times10^3$ m/s and $c_L = 5.14\times10^3$ m/s are, respectively, the sound velocities for TA and LA acoustic modes. The electron-phonon form factor is given by

$$I_{\nu\nu'}(q_\perp) = \int_{-\infty}^{\infty} e^{iq_\perp z} \psi_\nu(z)\psi_{\nu'}(z) dz \tag{23}$$

and shown in Fig. 9 for intra- and intersubband transitions in two subbands occupied by electrons. If we perform summation of Eq. (19) bearing in mind energy and momentum conservation laws, then the electron-phonon transition rate $\Gamma_\lambda(\vec{q},T)$ transforms to

$$\Gamma_\lambda(\vec{q},T) = \frac{Am^* c_\lambda}{2\pi\hbar^2\rho V\omega_q^2} |M_\lambda(\vec{q})|^2 \sum_\alpha G_{\alpha,\lambda}(q_\parallel,T) \times \left| \sum_\beta \varepsilon^{-1}_{\alpha,\beta}(q_\parallel) I_\beta(q_\perp) \right|^2, \tag{24}$$

where

$$G_{\nu\nu',\lambda}(q_\parallel,T)=\frac{\sqrt{2m^*}}{\hbar}\int_{E_{\min}}^{\infty}\frac{f_T(E+E_\nu)[1-f_T(E+E_\nu+\hbar c_\lambda q_\parallel)]dE}{\sqrt{E-\frac{\hbar^2}{2m^*}\left(\frac{m^*(E_{\nu'}-E_\nu)}{q_\parallel\hbar^2}+\frac{q_\parallel}{2}-\frac{m^*c_\lambda}{\hbar}\right)^2}}, \tag{25}$$

where $E_{\min}$ is determined from the condition when the denominator is equal to zero.

Phonon energy absorption rate by an electron system is determined from the following expression:

$$Q_\lambda(T)=\sum_{\vec{q}}\hbar\omega_{\vec{q}}n_\lambda(\vec{q},T)\Gamma_\lambda(\vec{q},T), \tag{26}$$

where $n_\lambda(\vec{q},T)$ is the distribution function of incident phonons. In the frames of acoustic mismatch theory[7] and assuming Planckian distribution of phonons in the metal heater film the distribution function of phonons emitted from the heater is determined by

$$n_0(q,T,T_h)\propto[(e^{\hbar\omega_q/k_BT_h}-1)^{-1}-(e^{\hbar\omega_q/k_BT}-1)^{-1}], \tag{27}$$

where T_h and T are the heater and substrate temperatures, respectively, and k_B is the Boltzmann constant. Here the heater temperature T_h is determined from Eq. (1). In order to establish the distribution function of incident phonons we have to take into account the processes of phonon scattering that occur during their propagation in the bulk of substrate. We restrict ourselves to isotope scattering and phonon-phonon scattering processes. Their scattering rates can be written as

$$\tau^{-1}_{\text{isotope}}(\omega)=A\omega^4, \tag{28}$$

$$\tau^{-1}_{\text{ph-ph}}(\omega,T)=B\omega^2T^3, \tag{29}$$

where $A=4.75\times10^{-45}$ s^3 and $B=3.6\times10^{-23}$ s/K^3 (see Refs. 15,16). Then the distribution function of phonons incident to the 2DEG for small incidence angles [when $\cos(\theta)\simeq1$] is given by

$$n_\lambda(q,T,T_h)=n_0(q,T,T_h)e^{-\tau^{-1}(\omega_q,T)L/c_\lambda}, \tag{30}$$

where L is the sample thickness and $\tau^{-1}(\omega_q,T)=\tau^{-1}_{\text{isotope}}(\omega_q)+\tau^{-1}_{\text{ph-ph}}(\omega_q,T)$ the total phonon scattering rate.

The total absorbed phonon power is given by

$$Q_\lambda(T,T_h)\propto\int d\Omega_q\int_0^\infty dq\,q^3n_\lambda(q,T,T_h)\Gamma_\lambda(\vec{q},T), \tag{31}$$

where any phonon focusing effects[17] are neglected. The integration over solid angle Ω_q is performed within the cone of incident phonons, which is determined by the phonon source size and its distance to the 2DEG.

VI. RESULTS OF CALCULATIONS AND DISCUSSION

Let us now turn to the results of numerical calculations of absorbed phonon power by the 2DEG in a δ structure. The calculations were performed for TA phonon absorption only and the maximum incidence angle of phonons was taken to be about 7°, which corresponds to the geometry of the experiment.

As it was already shown above (see Sec. V A), the considered electronic system consists of two occupied subbands; therefore, when calculating the absorbed phonon power we must take into account all possible intrasubband and intersubband electron-phonon transitions. The relative contributions from three strongest processes (1-1, 2-2, and 1-2) are presented in Fig. 10; the contributions from other processes with unoccupied subbands (1-3, 2-3, etc.) are negligibly small and not shown in this figure. Figure 10 shows that the main processes responsible for phonon energy absorption are intrasubband processes in occupied subbands (1-1 and 2-2 in our case) while intersubband processes (1-2 in our case) are not so important. Calculations show that in the case of unscreened electron-phonon interaction contributions from 1-1 and 2-2 processes are equal, while the introduction of screening reduces the relative contribution of the 1-1 process approximately by a factor of 2 (see Fig. 10). This means that the higher subband absorbs more than 70% of the energy accumulated by the 2DEG from the phonon flux although this subband possesses only 13% of all electrons. This can be explained by the fact that electrons in the second subband are less screened (due to lower electron density) by their spatial distribution; therefore the electron-phonon matrix element is greater for the 2-2 process than for the 1-1 process.

The total absorbed phonon power represented by the sum over all possible absorption processes according to Eqs. (24) and (31) as a function of ambient temperature is shown in Fig. 3(b). This figure also shows the experimental dependence of absorbed phonon power deduced from phonoconductivity data according to Eq. (9), i.e., $\delta Q_{\text{abs}}(T)\propto\delta\sigma(T)T^\gamma$.

The dependence of phonoconductivity on temperature can be obtained according to Eq. (9); it is shown in Fig. 2(a) by a solid line and reveals rather good agreement with experiment. This figure also shows the dependence of the phonoconductivity on electric power dissipated in the 2DEG that

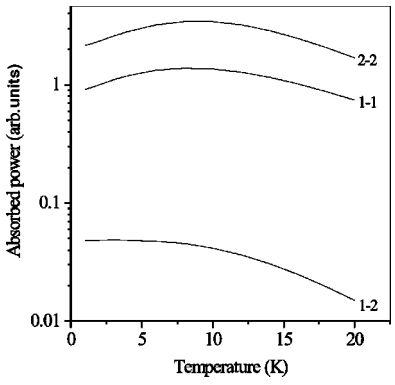

FIG. 10. Relative contribution to absorbed phonon power from intersubband and intrasubband electron transitions.

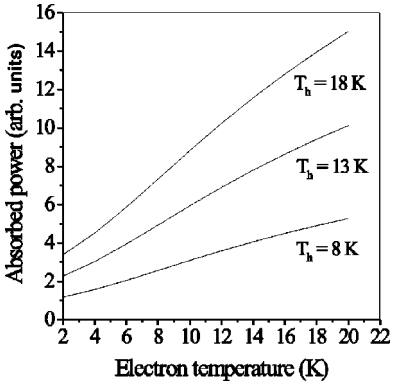

FIG. 11. The dependence of phonon-absorbed power on electron temperature.

can also be described by the model presented in this paper. The dependence of electron temperature on electric power $T_e(Q)$ is easy to get from the experimentally obtained energy loss rate [see Eq. (3)]. Therefore the dependence of $\delta\sigma$ on Q has the form [from Eq. (9)]

$$\frac{\delta\sigma(Q)}{G_0} = A\frac{\delta Q_{\rm abs}[T_e(Q)]}{T_e(Q)^{\gamma}}. \tag{32}$$

This formula actually describes the dependence of phonoconductivity on *electron* temperature T_e but not ambient temperature T as in Eq. (9). This means that the phonon flux, incident on the 2DEG, is independent of $T_e(Q)$ because phonon flux is determined only by heater temperature T_h and ambient temperature T. In this case the value of $\delta Q_{\rm abs}$ is determined by the temperature dependence of the electron-phonon transition rate $\Gamma_\lambda(\vec{q},T_e)$. The dependence $\delta Q_{\rm abs}(T_e)$ calculated for different heater temperatures and constant ambient temperature $T=2$ K is shown in Fig. 11.

The result of the calculation of the dependence of phonoconductivity $\delta\sigma$ vs input electric power Q with *no adjustable parameters* according to Eq. (32) is shown in Fig. 3(a) by a dashed line. This figure shows that the general behavior of calculated dependence agrees with what was observed in experiment but also a discrepancy at higher values of dissipated electric power Q is seen. Qualitatively, this can be accounted for by the fact that the higher energy subband is heated to higher temperatures than the lower subband by the same electric field.[18] For low values of heating electric power differences in temperature between different subbands are small and calculation agrees well with the experiment. However with increasing electric power this temperature difference begins to be more strongly pronounced and is observed as a deviation of experimental data from the calculated curve (which was obtained under the assumption of equal subband temperatures).

All phonoconductivity experiments discussed above were performed for a constant value of electric power dissipated in the heater. We have also carried out the experiment with constant ambient temperature and varying heater power, which determines heater temperature T_h (see Fig. 5).

Using our model we are also able to calculate the dependence of phonoconductivity on the temperature of heater film [see Eq. (31)] at constant ambient temperature. The result of this calculation for $T=2$ K is presented in Fig. 5 together with the relevant experimental data. One can see that the experimental data show constant increasing deviation from the calculated curve with decreasing heater temperature. This deviation means that the actual temperature of the heater was lower than the value, calculated according to acoustic mismatch theory [see Eq. (1)]. The highest heater temperatures correspond to the case when liquid helium around the heater film boils and heat transfer to helium is small. This means that almost all power goes to phonons that are emitted into the crystal.[8] If the power dissipated in the heater is not high enough to boil helium around the heater film, then the transfer of energy to helium is much stronger and must be taken into account in calculations of the heater temperature.

It is possible to estimate the energy δW accumulated in the 2DEG layer due to the absorption of nonequilibrium phonons: $\delta W = C\,\delta T$, where C is the heat capacity of 2DEG. For the heat capacity we use the Sommerfeld expansion[19] $C=\pi^2 k_B^2 D(E_{\rm F})T/3$, where $D(E_{\rm F})$ is the density of states at Fermi level $E_{\rm F}$. Having $\delta T\approx 0.4$ K for $T=2$ K one can easily estimate $\delta W\approx 3\times 10^{-13}$ J/cm^2, while the energy dissipated in the heater is $W_h=5\times 10^{-4}$ J/cm^2. This value δW is the difference between the energy absorbed from the phonon flux $\delta W_{\rm abs}$ and emitted to the lattice $\delta W_{\rm emit}$. The latter can be expressed via emission power $\delta Q_{\rm emit}$ as

$$\delta W_{\rm emit} = \tau_{\rm pulse}\delta Q_{\rm emit}$$

with $\tau_{\rm pulse}$ being the phonon pulse duration (see Sec. II). Then using Eq. (3) with $T_e = T+\delta T$ one can estimate $\delta W_{\rm emit}\approx 10^{-11}$ J/cm^2. Therefore the energy absorbed from phonon flux is also of the order of 10^{-11} J/cm^2 because the energy accumulated in the 2DEG (which is the cause of the temperature increase δT) is only few percent of the total absorbed energy.

VII. CONCLUSIONS

We have observed a positive phonoconductivity response in δ-doped GaAs that decreased with increasing heating of carriers and weak magnetic field. This effect is attributed to the temperature-dependent quantum corrections to conductivity that change their value upon absorption of phonon energy. The increase of electron temperature due to phonon absorption is calculated from the balance between the energy absorbed from phonon flux and emitted to the lattice by 2D electrons. The dependence of absorbed phonon energy on electron temperature was calculated using the self-consistent approach in determination of wave functions and including screening of the electron-phonon interaction in the random-phase approximation for the 2DEG with several subbands. The phonon emission rate was obtained experimentally from magnetotransport measurements of the weak localization effect.

Results of the model are in good agreement with experimental data. We believe it may be suitable for treating the phonon-assisted processes in other low-dimensional disordered electron structures.

ACKNOWLEDGMENTS

We gratefully acknowledge Professor O. Sarbey for many useful discussions and assistance in calculations. This work

was supported by the Ukrainian State Foundation for Basic Research (Grant No. 2.4/93).

APPENDIX A

We derive here the expression for the matrix dielectric function $\varepsilon_{\alpha,\beta}(q_\parallel)$ used for calculation of the electron-phonon matrix element [see Eq. (20)]. Here the notations for $\alpha=(\nu,\nu')$ and $\beta=(\mu,\mu')$ are the same as in Eq. (20). The general expression at arbitrary temperature in the random phase approximation is given by[20]

$$\varepsilon_{\alpha,\beta}(q,T)=\kappa\delta_{\alpha,\beta}+\frac{2\pi e^2}{q}\chi_\alpha(q,T)F_{\alpha,\beta}(q), \tag{A1}$$

where the polarization operator has the form

$$\chi_{\nu\nu'}(q,T)=-2\sum_{\vec{k}}\frac{f_T[E_\nu+E(\vec{k})]-f_T[E_{\nu'}+E(\vec{k}+\vec{q})]}{E_\nu+E(\vec{k})-E_{\nu'}-E(\vec{k}+\vec{q})} \tag{A2}$$

and the Coulomb form factor is given by

$$F_{(\nu\nu')(\mu\mu')}(q)=\int_{-\infty}^{\infty}dz\int_{-\infty}^{\infty}dz'\,\psi_\nu(z)\psi^*_{\nu'}(z)\psi_\mu(z')\times\psi^*_{\mu'}(z')e^{-q|z-z'|}. \tag{A3}$$

We consider only the contribution from the occupied subbands to the dielectric function because the contribution from the subbands lying above the Fermi level is negligible at low temperatures ($T\ll E_{F\nu}$ where ν numerates occupied subbands only).[21] In the case of long-wavelength phonons ($q<k_{F\nu}+k_{F\nu'}$, where $k_{F\nu}$ is the Fermi wave vector of νth subband) and for low temperatures the expression for the polarization operator reduces to

$$\chi_{\nu\nu'}(q,T)=\frac{m^*}{\pi\hbar^2}. \tag{A4}$$

Therefore the dielectric function of the system with N occupied subbands is approximated by a $N^2\times N^2$ matrix given by

$$\varepsilon_{\alpha,\beta}(q)=\kappa\delta_{\alpha,\beta}+\frac{2m^*e^2}{q\hbar^2}F_{\alpha,\beta}(q). \tag{A5}$$

[1] P. A. Lee and T. V. Ramakrishnan, Rev. Mod. Phys. **57**, 287 (1985).
[2] G. Bergmann, Phys. Rep. **101**, 1 (1984).
[3] M. Blencowe, J. Phys.: Condens. Matter **8**, 3121 (1996).
[4] A. Kent *et al.*, Phys. Rev. B **55**, 9775 (1997).
[5] G. M. Gusev *et al.*, Fiz. Tekh. Poluprovodn. **25**, 601 (1991) [Sov. Phys. Semicond. **25**, 364 (1991)].
[6] M. Asche, K.-J. Friedland, P. Kleinert, and H. Kostial, Semicond. Sci. Technol. **7**, 923 (1992).
[7] W. A. Little, Can. J. Phys. **37**, 334 (1959).
[8] B. A. Danilchenko and V. M. Poroshin, Cryogenics **23**, 546 (1983).
[9] B. Altshuler, A. Aronov, A. Larkin, and D. Khmelnitsky, Zh. Éksp. Teor. Fiz. **81**, 768 (1981) [Sov. Phys. JETP **54**, 411 (1981)].
[10] P. A. Lee and T. V. Ramakrishnan, Phys. Rev. B **26**, 4009 (1982).
[11] A. M. Kreschuk *et al.*, Solid State Commun. **65**, 1189 (1988); Fiz. Tekh. Poluprovodn. **22**, 604 (1988) [Sov. Phys. Semicond. **22**, 377 (1988)].
[12] J. P. Perdew and A. Zunger, Phys. Rev. B **23**, 5048 (1981).
[13] C. R. Proetto, in *Delta-doping of Semiconductors*, edited by E. F. Shubert (Cambridge University Press, Cambridge, 1996).
[14] V. Karpus, Fiz. Tekh. Poluprovodn. **22**, 43 (1988) [Sov. Phys. Semicond. **22**, 27 (1988)].
[15] S. I. Tamura, Phys. Rev. B **31**, 2574 (1985).
[16] B. Mogilevskiy and A. Chudnovskiy, *Thermal Conductivity of Semiconductors* (Nauka, Moscow, 1972) (in Russian).
[17] J. P. Wolfe, *Imaging Phonons* (Cambridge University Press, Cambridge, 1998).
[18] V. Kubrak, P. Kleinert, and M. Asche, Semicond. Sci. Technol. **13**, 277 (1998).
[19] Q. Li, X. C. Xie, and S. Das Sarma, Phys. Rev. B **40**, 1381 (1989).
[20] E. D. Siggia and P. C. Kwok, Phys. Rev. B **2**, 1024 (1970).
[21] G. Q. Hai, N. Studart, and F. M. Peeters, Phys. Rev. B **52**, 8363 (1995); L. R. Gonzalez, J. Krupski, and T. Szwacka, *ibid.* **49**, 11 111 (1994).